scientific reports

Check for updates

OPEN

Detection of vital signs based on millimeter wave radar

Zhanjun Hao[1,2]✉, Yue Wang[1], Fenfang Li[1], Guozhen Ding[1], Kai Fan[1] & Yifei Gao[1]

With the growing demand for health monitoring, non-contact vital signs monitoring technology has garnered widespread attention. While traditional health monitoring methods are accurate, they have limitations in terms of non-contact and non-invasive capabilities. This paper proposes a non-contact vital signs monitoring method based on frequency modulated continuous wave (FMCW) millimeter-wave radar, named MRVS, to enhance both convenience and accuracy. The method consists of three steps: signal processing, decomposition, and reconstruction. Firstly, the millimeter-wave radar is used to detect chest movements, extracting both respiration and heartbeat signals. Then, combining signal superposition with phase difference techniques effectively eliminates static clutter and respiratory harmonic interference, enhancing the signal. Next, discrete wavelet transform (DWT) is utilized to suppress clutter and noise further, performing signal decomposition. The reconstruction module employs an adaptive Kalman filter (AKF) combined with square root normalization for accurate heart rate estimation. Experimental results demonstrate that this method achieves an estimation error rate of less than 7% under different distances, angles, and postures, showcasing high accuracy and robustness and providing a new solution for non-contact vital signs monitoring.

Keywords Vital signs, Millimeter-wave radar, DWT, AKF, Heart rate estimation

With the advancement of society and the growing concern for health, monitoring human vital signs[1] has become an urgent issue in the medical field. Traditional health monitoring methods mainly rely on wearable devices, such as respiratory belts[2] and ECG sensors[3,4]. While these methods provide relatively accurate results, they have certain limitations in terms of non-contact and non-invasive monitoring. To address these limitations, non-contact vital signs monitoring techniques[5–9] have increasingly attracted the attention of researchers in recent years.

Existing vital signs monitoring methods utilize computer vision, acoustic signals, and radio frequency (RF) signals. Computer vision-based methods have high environmental requirements and pose privacy risks. Acoustic signals offer potential for monitoring vital signs, but their range is limited. RF signals, however, can effectively address these issues. As a result, most current research focuses on using RF signals to detect the vibrations caused by chest movements, enabling non-contact monitoring of respiration and heartbeat. Wi-Fi-based sensing techniques have also seen significant applications in recent years, such as in personnel positioning[10] and respiratory monitoring[11,12]. However, Wi-Fi operates in the 2.4/5 GHz frequency bands, with narrow bandwidth, limited antennas, and a longer wavelength, making it particularly challenging to detect heartbeat signals using Wi-Fi.

Radar technology, which uses electromagnetic waves to detect and locate objects, offers advantages such as strong penetration, non-invasiveness, and low environmental sensitivity, making it more suitable for monitoring human vital signs[13]. Currently, three main types of radars are used for vital signs monitoring in the literature: continuous wave (CW) Doppler radar, ultra-wideband (UWB) radar, and frequency-modulated continuous wave (FMCW) radar. Dong et al.[14] utilized CW Doppler radar to detect heartbeat signals by sensing movements on the back of the human body. However, due to the absence of modulated spectral information, CW radar is highly susceptible to clutter interference, leading to poor accuracy in vital signs detection. In contrast, both UWB and FMCW radars feature wider bandwidths and can provide distance information about the target, making them more suitable for monitoring vital signs. For example, a method combining UWB radar with time-varying filters was proposed in the literature[15] to monitor both respiration and heartbeat. Although this approach can extract vital signs, UWB radar suffers from high hardware costs and significant energy consumption.

In contrast, FMCW radar, with its high distance and velocity resolution, is more effective at extracting target micro-motion information and performs particularly well in vital signs detection[16–19]. Based on this, this paper

[1]College of Computer Science and Engineering, Northwest Normal University, Lanzhou 730070, Gansu, China. [2]Gansu Province Internet of Things Engineering Research Center, Northwest Normal University, Lanzhou 730070, China. ✉email: haozhj@nwnu.edu.cn

proposes a vital signs monitoring method, MRVS, using FMCW radar, aiming to provide higher accuracy and robustness.

However, while traditional methods based on discrete wavelet transform (DWT) are commonly used for the decomposition and reconstruction of respiratory signals in vital signs processing, they have limitations in extracting heartbeat signals. This is primarily because the respiratory frequency is lower and more stable, making DWT particularly effective at capturing low-frequency components. As a result, earlier studies focused more on using DWT for respiratory frequency estimation[20]. However, since heartbeat signals have a higher frequency and smaller amplitude, DWT's ability to resolve these signals is relatively weak. Although some studies have applied pre-filtering techniques to reduce interference from respiratory signals, the improvement mainly lies in signal separation, and the accuracy of heartbeat signal extraction still requires enhancement[21].

To address the above issues, this paper proposes a signal processing framework that combines adaptive Kalman filtering and square root normalization: Firstly, the millimeter wave radar is used to sense the person's chest movement signals, including the respiratory and heartbeat signals. In this part, the positioning of the human chest is realized, and then the phase information of vital signals is extracted along slow time. Secondly, the signal processing module enhances the signal by overlaying the signals combined with phase differencing to eliminate the interference of static clutter and breathing harmonics. Again, discrete wavelet transform is used to suppress clutter and noise further. Finally, the signal is reconstructed by combining adaptive Kalman filtering and square root normalization for accurate heart rate estimation.

The main contributions of this paper can be summarized as follows:

1. Aiming at the problem that heartbeat sensing signals are easily submerged in noise, a heartbeat signal enhancement method based on signal superposition combined with differential is proposed, effectively highlighting the chest displacement signals induced by heartbeat motion during the sensing process.
2. The vital signal decomposition and reconstruction strategy based on AKF and DWT combines the fusion denoising technique to achieve accurate and effective signal separation.
3. The performance of the proposed method was evaluated in the presence of multiple influencing factors. The experimental results show that MRVS can effectively suppress clutter interference, and the estimation error rate is less than 7% under different poses and angles.

Related Work

This section reviews recent advances in vital signs monitoring from three perspectives: conventional filter-based, modal decomposition-based, and wavelet transform-based solutions.

Conventional filter-based solutions

Separating vital signals is a core issue in the field of human vital signs monitoring using millimeter-wave radar[22–24]. To improve signal quality and accuracy, many early researchers adopted filter-based methods for separating and denoising biological signals. Filter techniques have been widely applied in signal processing in existing studies. Previous research has shown that signals such as heartbeat and respiration typically have different frequency components. Kim et al.[25] designed a low-cost, non-contact phase-monitoring radar that used a digital bandpass filter to separate respiration and heartbeat, but the effective testable distance was limited to 40 cm. In[26], the Opal radar system was developed to estimate the respiratory rate of postoperative patients, achieving an error within two breaths. Anitori et al.[27] used a new compact X-band FMCW radar to select the optimal frequency for observing vital signs. In[28], techniques such as Fast Fourier Transform, Savitzky-Golay filter, Elliptic filter, and Kalman filter were employed to separate respiratory and heartbeat signals. However, none of these methods can accurately estimate heart rate when respiratory signals are present. As a result, subsequent researchers began introducing modal decomposition methods to achieve more accurate heart rate monitoring.

Mode decomposition-based solutions

Mode Decomposition is an adaptive processing method for non-smooth and non-linear signals[29], which can decompose non-smooth signals into stable modal components and extract effective frequency information to produce clear spectrograms. To solve the problem of mutual interference between respiratory and heartbeat signals as well as ambient noise, the methods commonly used by many researchers nowadays include the Empirical Mode Decomposition (EMD) algorithm[30], the Variational Mode Decomposition (VMD) algorithm[31].

Yang et al.[32] proposed a vital signs extraction method based on the integrated empirical modal decomposition (EEMD) algorithm to adaptively decompose the restructured signals, which can quickly extract a respiratory heartbeat. However, the EMD algorithm produces the problem of mode mixing during the decomposition process[33], which can lead to a decrease in heart rate estimation accuracy due to the influence of respiratory harmonics. Xu et al.[34] designed a hierarchical variational modal decomposition (VMD) method to extract and estimate the fundamental cardiac motions in the millimeter-wave signals, which is used to accurately estimate the driver's heart rate and heartbeat cycle in a dynamic driving environment. It is demonstrated that the VMD can effectively overcome the modal mixing problem. However, selecting the appropriate number of decomposition layers K and the penalty factor α remains a critical challenge for the algorithm.

Wavelet decomposition-based solutions

Wavelet transform (WT) is widely used for vital signal extraction because it inherits the localization idea of short-time Fourier transform (STFT) and overcomes the limitation of a fixed window, offering a time–frequency window that adapts with frequency. He et al.[35] proposed an improved WT-based method for heartbeat signal extraction in non-contact vital sign monitoring. Compared to the EMD and bandpass filtering methods, this approach offers higher accuracy in heartbeat rate monitoring. Wang et al.[36] developed a compressed sensing

Vital signs	Frequency	Front	Back
		Amplitude	
Breathing rate	0.1–0.5Hz	~1–12 mm	~0.1–0.5 mm
Heart rate	0.8–2.0Hz	~0.1–0.5 mm	~0.01–0.2 mm

Table 1. Frequency and amplitude of respiration and heartbeat in adults.

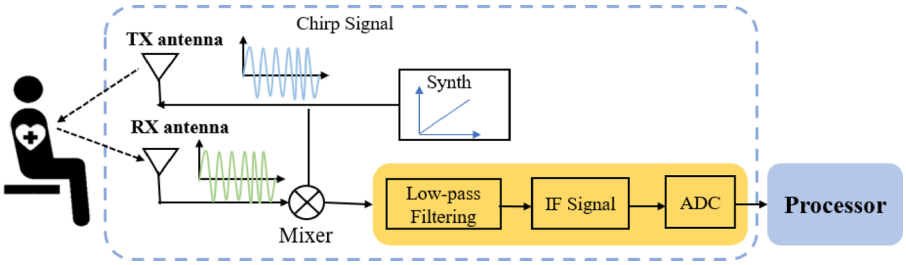

Fig. 1. Millimeter-wave radar detection of vital signals principle.

algorithm based on orthogonal matching pursuit and an adaptive soft-threshold denoising algorithm using discrete wavelet transform to separate and reconstruct respiratory and heartbeat signals. This method effectively suppresses noise and harmonic interference, achieving an accuracy of up to 93%. Liu et al.[37] used wavelet analysis and autocorrelation to extract high-precision heart rate parameters. Although wavelet transform allows for simultaneous analysis of physiological signals in both the time and frequency domains, effectively separating respiratory and heartbeat signals, selecting an appropriate wavelet basis function remains a crucial challenge.

Conventional filters can address signal frequency separation to some extent in vital signs monitoring, but they are less effective when dealing with non-stationary signals and lack adaptivity. While modal decomposition methods offer advantages in processing nonlinear and non-stationary signals, they are prone to modal aliasing in environments with complex frequency components and high noise, and the computational complexity is high. In response to these limitations, this paper proposes a method using discrete wavelet transform (DWT) for more effective separation of respiratory and heartbeat signals through multiresolution analysis and adaptive processing, thereby significantly improving the accuracy of vital signs monitoring.

Preliminaries

Human respiration is accomplished by the periodic stretching and contracting of the diaphragm and pectoral muscles; similarly, heartbeat activity is accomplished by the periodic stretching and contracting of the heart, so the two signals can be approximated to be modeled as sinusoidal signals[38]. In general, the amplitude and frequency of human respiration and heartbeat are shown in Table 1.

The basic principle of millimeter wave radar for detecting vital signs is to sense the small vibrations caused by the rise and fall of the chest through the signal. The radar transmits electromagnetic waves of specific waveforms to irradiate the moving chest wall and generate echoes. The chest displacement information containing respiratory and heartbeat parameters is obtained by demodulating the echoes after Doppler modulation of the human chest wall. The basic principle is shown in Fig. 1.

Based on the above information and assuming that the human body is stationary to the radar, the vital sign signals and their echo signals under the FMCW radar can be modeled. The radar-detected respiratory and heartbeat signals can be approximately represented as sinusoidal signals:

$$R_B(t) = r_1 \sin(2\pi f_1 t) \tag{1}$$

$$R_H(t) = r_2 \sin(2\pi f_2 t + \theta) \tag{2}$$

where $r_1 \sin(2\pi f_1 t)$ is the respiratory signal, r_1 denotes the respiratory signal vibration amplitude, and f_1 is the respiratory signal frequency. Similarly, $r_2 \sin(2\pi f_2 t)$ is the heartbeat signal, r_2 denotes the heartbeat signal vibration amplitude, and f_2 is the heartbeat signal frequency, θ denotes the phase difference that exists between the heartbeat signal and the respiratory signal. Convert Eqs. (1), (2) to discrete form respectively:

$$R_B(m) = r_1 \sin\left(\frac{2\pi f_1 (m-1)}{prf}\right) \tag{3}$$

$$R_H(m) = r_2 \sin\left(\frac{2\pi f_2 (m-1)}{prf} + \theta\right) \tag{4}$$

where m is the discrete sampling point and prf is the sampling frequency when the data is discretised.

Thus, the vital sign signaling model can be written as:

$$R(m) = R_0 + r_1 \sin\left(\frac{2\pi f_1(m-1)}{prf}\right) + r_2 \sin\left(\frac{2\pi f_2(m-1)}{prf} + \theta\right) \tag{5}$$

where R_0 is the perturbation signal, and the perturbation signal mainly includes noise perturbation signal and body slight perturbation signal. The sampling time T_S is $1/prf$, then the human physiological signal model can be expressed as:

$$R(mT_S) = R_0 + r_1 \sin(2\pi f_1(m-1)T_S) + r_2 \sin(2\pi f_2(m-1)T_S + \theta) \tag{6}$$

After that, the mixer combines the transmit antenna TX and receive antenna RX signals to generate an intermediate frequency (IF) signal. Since the FMCW radar system obtains the distance, speed, and angle of the object under test by capturing the reflected signals, it is possible to differentiate between respiration and heart rate by calculating the vibration amplitude and frequency, i.e., the phase change.

Proposed method

Overview

In this section, the proposed method, MRVS, based on millimeter wave radar, is described in detail, and the flow is shown in Fig. 2. The process consists of three parts: signal processing and enhancement, vital signal decomposition, and signal reconstruction. The signal processing part extracts the phase information from the human chest displacement information acquired by the millimeter wave radar. Signal overlay suppresses static noise and enhances the heartbeat signal by combining it with a first-order difference. The vital signal decomposition part uses wavelet decomposition for cardiac motion pattern extraction to accurately extract the respiratory heartbeat signal from the complex chest motion. Finally, the PSD of the corresponding layer signals is calculated, and the obtained two sets of signals are reconstructed separately using AKF to estimate heart rate accurately.

Signal processing

The phase of the IF signal obtained after mixing the transmit and receive signals of the radar is equal to the phase difference between the transmit and receive signals. It is, therefore, also a sinusoidal function, which can be expressed as:

$$IF_{out} = \sin[(f_1 - f_2)\,t + (\varphi_1 - \varphi_2)] \tag{7}$$

Extracting vital signs information from the frequency variations of intermediate frequency (IF) signals poses challenges due to the high operating frequency of FMCW millimeter-wave radars and the limitations in hardware sampling points. At high frequencies, the amplitude of frequency changes is small, resulting in lower extraction accuracy and making the signal more susceptible to noise and external interference. In contrast, phase signals are more sensitive to minute displacements of the target, offering higher precision and reliability in detecting subtle movements of the human body, such as breathing and heartbeat. Therefore, compared to frequency information, phase signals exhibit more significant advantages in vital signs extraction, particularly for high-precision measurements.

In order to extract the features of respiration and heartbeat, we need to detect the phase change of the target FMCW signal within the range bin. The specific process begins with performing a one-dimensional Fourier transform (FFT) on the IF signal, as shown in Fig. 3a. Through FFT analysis, the distance of the target can be

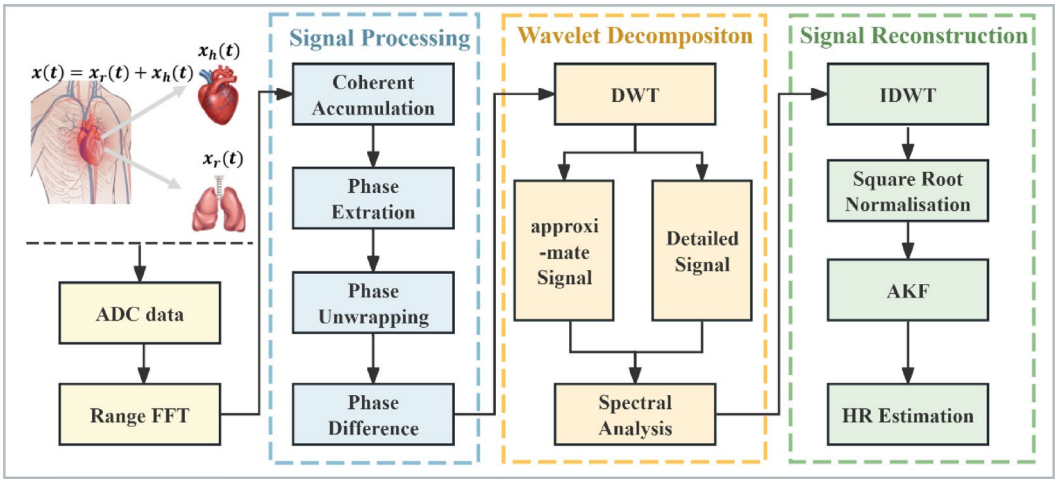

Fig. 2. Overview of MRVS.

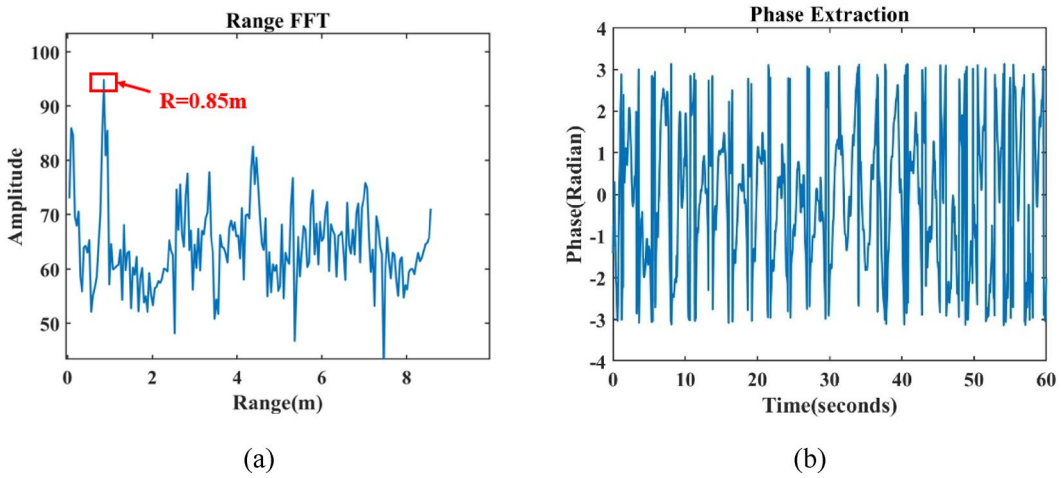

Fig. 3. Get phase (**a**) Range FFT (**b**) Phase.

determined, and the corresponding range bin is identified, which becomes the focus area for subsequent phase extraction. Based on the phase variation of this range bin, we can measure the phase changes caused by small chest vibrations, and the calculation formula is as follows:

$$\Delta\emptyset_b = \frac{4\pi}{\lambda}\Delta d \tag{8}$$

where Δd is the slight change in the thoracic cavity caused by the human body during breathing and heartbeat, and λ is the wavelength. As shown in Fig. 3b, the obtained phase information illustrates the phase variation over time. However, due to ambient noise, motion interference, and hardware limitations, discontinuities may appear in the extracted phase signals. These discontinuities must be further processed and analyzed to ensure that the periodic changes in respiration and heartbeat are accurately captured.

In millimeter-wave radar monitoring systems, minute thoracic displacements caused by cardiac activity are often masked by dominant respiratory motion. Effectively separating and enhancing the heartbeat component remains one of the key challenges. Prior studies have shown that periodic cardiac signals can still be detected by radar under breath-holding conditions, confirming the feasibility of using millimeter-wave radar to sense subtle cardiac-induced motions. Moreover, some studies have further validated the physiological origin of these signals through comparative experiments with electrocardiography (ECG)[39,40].

To address potential issues in the phase extraction process and to further improve the accuracy of vital sign detection, this study proposes a multi-stage signal processing approach, which consists of the following three steps:

Firstly, the signal is processed using the coherent accumulation method and compared with the denoising effects of the mean-phase cancellation method and the Moving Target Indication (MTI) algorithm. Prior to these steps, a DC offset removal procedure was applied to eliminate the constant bias within the signal, thereby enabling more accurate extraction of periodic components. Additionally, this step helps mitigate the influence of low-frequency drift. Figure 4a shows the raw unprocessed signal, with a signal-to-noise ratio (SNR) of 7.56 dB, exhibiting significant noise interference. Figure 4b presents the result of the mean-phase cancellation method, which improves the SNR to 9.49 dB. Although this method reduces noise to some extent, its denoising effect still needs improvement, and the improvement in signal quality is limited. Figure 4c shows the denoising effect of the MTI algorithm, where the SNR is further enhanced to 13.8 dB, indicating that most noise has been effectively suppressed, though a small amount of clutter remains. Finally, Fig. 4d demonstrates the denoising effect of the coherent accumulation method proposed in this paper, achieving an SNR of 15.36 dB. This result shows that the method can effectively eliminate static background noise and significantly improve signal quality. It proves that the coherent accumulation method significantly removes static clutter, maximizing the clarity of vital signs signals.

Secondly, phase unwrapping is a crucial step when processing respiration and heartbeat data from millimeter-wave radar. Since the phase signal is constrained within the range of [0, 2π], phase wrapping can occur, leading to phase jumps that hinder the accurate capture of actual phase changes. In order to restore phase continuity, phase unwrapping is performed by calculating the phase differences between neighboring sampling points and detecting jumps exceeding π. When such a jump is detected, the phase value is adjusted by adding or subtracting 2π to ensure signal continuity. This process helps recover the proper frequency and amplitude information of the signal, thereby improving the accuracy of respiration and heartbeat estimation. Figure 5a illustrates the results after phase unwrapping, where the signal appears more continuous and smooth.

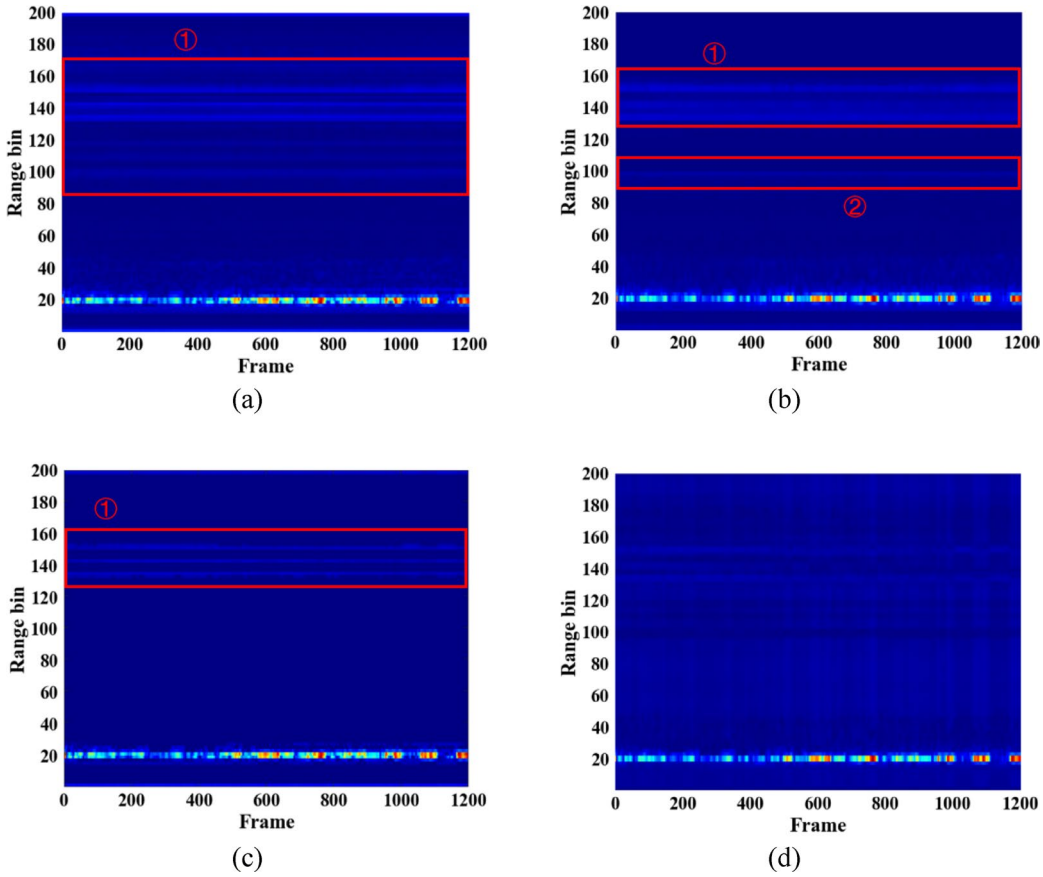

Fig. 4. Comparison of denoising methods (**a**) Original signal (**b**) Mean square offset (**c**) Moving target indication (**d**) Coherent accumulation.

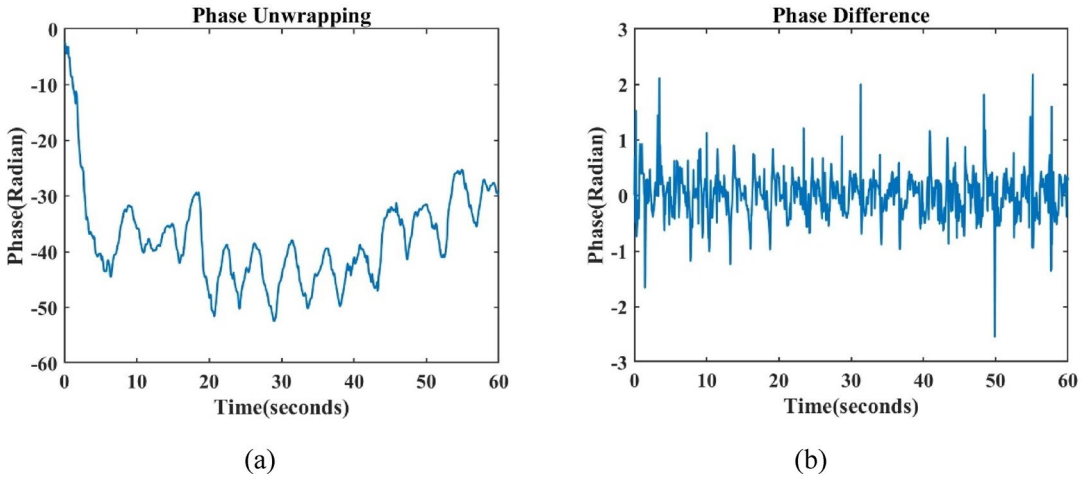

Fig. 5. Phase processing (**a**) Unwrapped phase (**b**) Phase difference.

Finally, in the resting state, the human body does not only generate rhythmic movements such as breathing and heartbeat, but may also include non-periodic components like muscle micro-movements and occasional posture adjustments. These interfering signals usually appear in the time–frequency domain as low-amplitude and unstable features. Therefore, to further enhance the heartbeat signal and reduce phase drift, this paper

Parameters	Orthogonality	Symmetry	Vanishing moment		Support length
			Scale function	Wavelet function	
Haar	Yes	Yes	No	1	1
Daubechies (db)	Yes	No	No	N	2N-1
BiorSpline (bior)	No	Yes	No	Nr-1	Decompose 2Dd + 1 Reconstruct 2Nr + 1
Symlets (sym)	Yes	Proximate	No	2N	6N-1
Coiffets (coif)	Yes	Proximate	2N-1	2N	2N-1

Table 2. Wavelet-based parameter indicators.

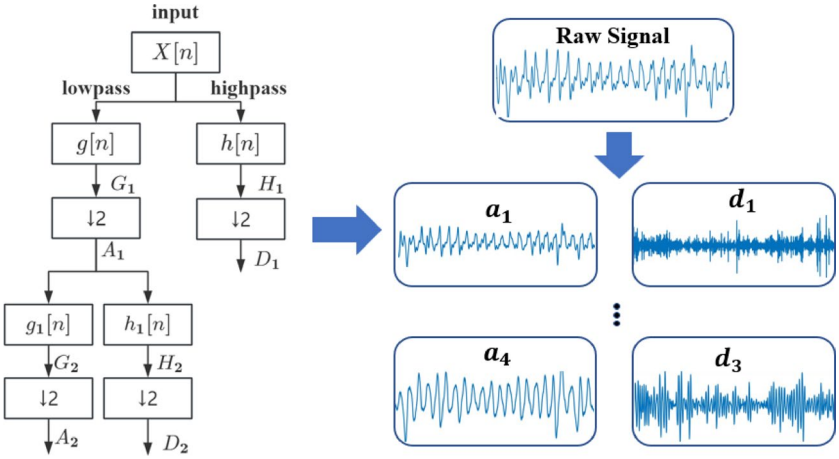

Fig. 6. DWT.

performs a differentiation operation on the unfolded phase. The differential processing can better emphasize the subtle changes in the heartbeat signal and effectively suppress potential phase drift issues. Figure 5b shows the result after differential processing, demonstrating that this method has a significant effect on heartbeat signal extraction.

Wavelet decomposition

To accurately and effectively analyze vital signs signals, this paper employs the wavelet transform method to decompose the signals. In wavelet transform, the choice of wavelet basis is crucial. Table 2 presents the parameter indicators for different wavelet bases. Among the commonly used wavelet bases, the Haar wavelet exhibits orthogonality and compact support. However, due to its lack of smoothness, it is typically suitable for processing discrete and abrupt signals rather than smooth vital signs signals. Though the Biorthogonal possesses biorthogonality and compact support, it may introduce redundant information due to the use of different wavelet bases for decomposition and reconstruction, potentially affecting the accuracy of signal decomposition and reconstruction. Symlets and Coiflets wavelets, with their better smoothness and approximate symmetry, are more suitable for processing symmetric signals. However, vital signs signals are not perfectly symmetric, and the higher-order design of these wavelets increases computational complexity.

In contrast, the Daubechies (db) wavelet basis lacks symmetry, but its orthogonality ensures the independence of signals across different frequency bands, enabling distortion-free signal reconstruction. Additionally, the Daubechies wavelet basis has high vanishing moments, allowing it to effectively separate high-frequency and low-frequency components and provide stronger noise suppression when processing complex signals with varying frequency characteristics, such as breathing and heartbeat signals. Therefore, despite its lack of symmetry, the db wavelet is the best choice for vital signs signal processing due to its excellent properties, including strong orthogonality, high vanishing moments, and suitable support length.

In this paper, we selected the Daubechies 5th-order wavelet (db5) for a four-level decomposition. This choice was made because db5 while ensuring computational efficiency, is capable of capturing the primary features of the signal. The four-level decomposition provides sufficient detail and approximation levels, making it well-suited for handling multi-scale physiological signals. This combination allows for the retention of key information when decomposing complex signals while avoiding unnecessary computational overhead, achieving an optimal balance between accuracy and efficiency.

In general, heart rate and respiration rate can be estimated after extracting phase information from vital signals. However, while heartbeat and respiration signals exhibit approximate periodic characteristics, harmonic

frequencies and noise often prevent these signals from taking on an ideal sinusoidal form. This allows the primary heartbeat and respiration frequencies to be easily masked by harmonics or noise, leading to significant estimation errors. Phase difference processing can make the heartbeat frequency more prominent, but in cases of non-periodic respiratory signals, harmonic peaks are often larger than the heartbeat frequency peaks. This can cause errors in heartbeat and respiration rate estimation using FFT methods and time-domain autocorrelation methods. To address these challenges, this paper proposes a method based on adaptive Kalman filtering and discrete wavelet transform (AKF-DWT) to separate and reconstruct heartbeat and respiration signals effectively.

Figure 6 illustrates the decomposition method used in this paper, and the DWT can be described as:

$$\mathrm{W_l n} = \sum_{k=-\infty}^{\infty} x\,(k) \cdot l\,(2n-k) \tag{9}$$

$$\mathrm{W_h n} = \sum_{k=-\infty}^{\infty} x\,(k) \cdot h\,(2n-k) \tag{10}$$

where $\mathrm{W_l n}$ is the low frequency (approximation) coefficient after decomposing the signal and $\mathrm{W_h n}$ is the high frequency (detail) coefficient after decomposing the signal. $x\,(k)$ denotes the discrete difference phase information, k is the number of sampling points, and n is the number of sampled data. $l\,(2n-k)$ and $h\,(2n-k)$ are the decomposition coefficients for the low-pass and high-pass filters of the wavelet analysis filter, respectively. After the finite order decomposition of $x\,(k)$, the overall signal can be reconstructed by the Inverse Discrete Wavelet Transform (IDWT).

$$R\mathrm{k} = \sum_{n=a}^{b} W_l\,(n) \cdot L\,(2n-k) + \sum_{n=a}^{b} W_h\,(n) \cdot H\,(2n-k) \tag{11}$$

where n is the index of the sampling point, a is the scale factor, and b is the displacement factor. $L\,(2n-k)$ and $H\,(2n-k)$ are the low-pass and high-pass reconstruction coefficients of the scale function and wavelet function. The decomposed approximation coefficients and detail coefficients can reconstruct the corresponding respiration and heartbeat signals in two groups.

Signal reconstruction

Power spectral density (PSD) shows the energy distribution of the signal in the frequency domain, which allows a better view of the respiratory and heartbeat frequencies and their harmonics. Therefore, in this paper, we use DWT to perform PSD analysis for each relevant approximation coefficient and detail coefficient to confirm the frequency distribution of heartbeat and respiration. Through signal decomposition as well as spectral estimation, we determined that the heartbeat signal mainly exists in layer D3. In contrast, the respiration signal mainly exists in layer A4, and the PSD for the respiration and heartbeat signals are shown in Fig. 7.

In the signal reconstruction stage, we first extracted the wavelet reconstruction coefficients of the corresponding layers and performed an inverse wavelet transform to reconstruct the respiratory and heartbeat signals. Subsequently, the separated respiratory and heartbeat signals were smoothed using adaptive Kalman filtering (AKF), which dynamically estimates the noise covariance to adapt to the non-stationary characteristics of the signals. This allows the AKF to effectively handle the dynamic changes and potential non-linear characteristics of the signals. Finally, combined with Algorithm 1, the respiratory and heartbeat signals were reconstructed, with the reconstruction results shown in Fig. 8.

To estimate the respiratory rate and heart rate more accurately, we identified the dominant frequencies of the heartbeat and respiratory signals by detecting the maximum amplitude in the power spectrum of the reconstructed signals and calculated the heart rate and respiratory rate based on these frequencies. To ensure the reliability of the detection results, we introduced a confidence threshold. If the maximum amplitude in the spectrum falls below the set threshold, the heartbeat signal is inferred to be invalid; otherwise, the heart rate is calculated using the corresponding frequency index. To further improve computational accuracy, the heart rate estimation was adjusted by incorporating the time difference between successive chirps in the signal.

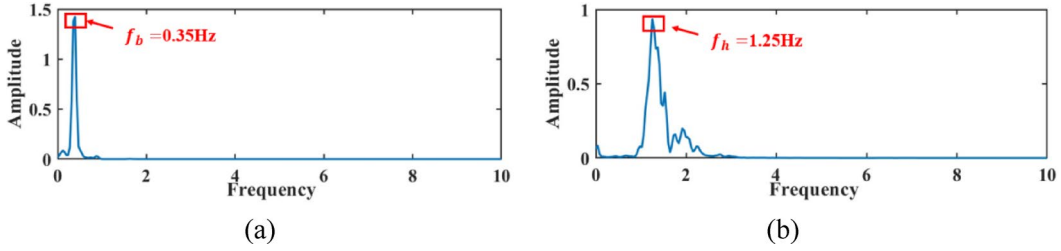

Fig. 7. Spectral analysis (**a**) Spectrogram of respiratory signals (**b**) Spectrogram of heartbeat signals.

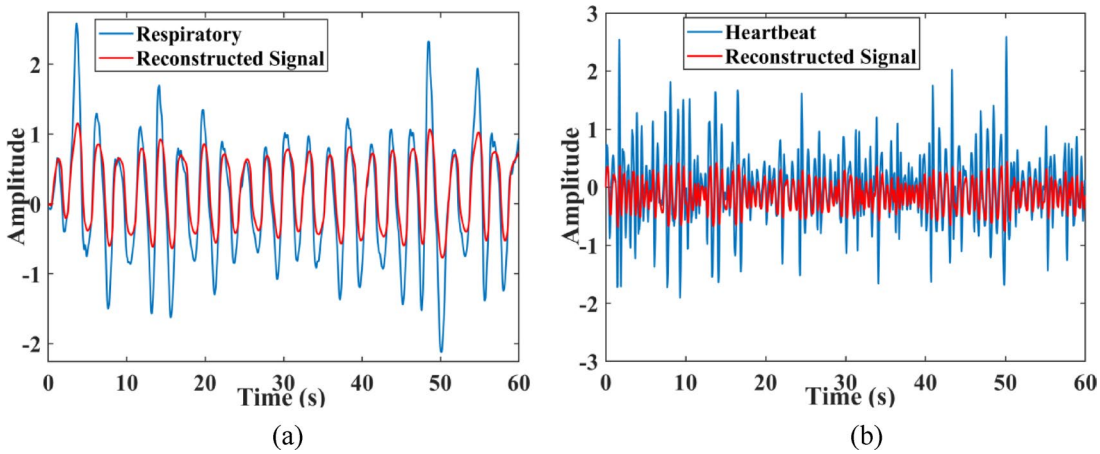

Fig. 8. Noise reduction reconstruction results for sub-signals (**a**) Respiratory signal (**b**) Heartbeat signal.

Threshold	Without noise	With noise	
	Estimated error rate (%)	False positive rate (%)	False negative rate (%)
0.001	2.8	10	12
0.01	3.0	6	7
0.1	2.7	5	10

Table 3. Comparison of the effect of different thresholds.

During the selection of the confidence threshold, experimental data was collected from different environments, including scenarios with and without heartbeat signals. Various levels of noise were introduced to increase the complexity of the detection task. The experiment determined the presence of a heartbeat signal by calculating the maximum amplitude of the signal, and different confidence thresholds were tested. If the maximum amplitude exceeded the threshold, the system would calculate the heart rate; if it fell below the threshold, the system would determine that there was no valid heartbeat signal. We evaluated the performance of each threshold by measuring the False Positive Rate (FPR) and the False Negative Rate (FNR) as shown in Table 3. FPR represents the proportion of cases where the system incorrectly detected a heart rate in the absence of a heartbeat signal, while FNR represents the proportion of cases where the system failed to detect a heart rate when a heartbeat signal was present.

The experimental results showed that in a noise-free environment, the performance across different thresholds was similar. However, under noisy conditions, lower thresholds tended to introduce more false positives, whereas higher thresholds resulted in more false negatives. After considering the accuracy of detection, the FPR, and the FNR, a threshold of 0.01 was determined to perform best in complex environments, maintaining robust heart rate detection even under noisy conditions. Therefore, 0.01 was chosen as the optimal threshold.

To ensure that the amplitude characteristics of the reconstructed signal remain consistent with the original signal, we applied square root normalization to the reconstructed signal. This method standardizes the energy of the reconstructed signal, maintaining consistency with the original signal in both the time and frequency domains. This approach enables accurate separation and reconstruction of the respiration and heartbeat signals, ultimately restoring the true respiration and heart rates. The specific formula for heart rate calculation is as follows:

$$Heart\ Ratebpm = \left(\frac{fs * \left(\frac{numFrame}{2} - (heart_{index} - 1) \right)}{numFrame} \right) * 60 \tag{12}$$

where fs is the sampling frequency, $numFrame$ is the number of frame, and $heart\_index$ is the frequency index corresponding to the maximum amplitude found in the power spectrum. We further adjusted the heart rate estimation by calculating the time difference between successive chirps in the signal to ensure the accuracy of the frequency estimation.

Input: Approximation coefficients from DWT approx_4, Detail coefficients detail_3.

Output: reconstructed signal

1: Initialize state $\hat{x}_0 = \begin{bmatrix} approx_4(1) \\ detail_3(1) \end{bmatrix}$, error covariance $P_0 = I_2$.

Set noise parameters $Q = 0.002$, $R_{min} = 0.005$, $R_{max} = 0.02$, $P_{min} = 0.001 * I_2$.

2: Kalman Filtering

for each sample k**=1 to** N **:**

a. Adjust $R_k = max(R_{min}, min(R_{max}, |(approx_4(k) - detail_3(k)|))$;

b. Calculate the Kalman gain, $K_k = P_{k-1}(P_{k-1} + R_k)^{-1}$;

c. Update $\hat{x}_k = \hat{x}_{k-1} + K_k(\begin{bmatrix} approx_4(k) \\ detail_3(k) \end{bmatrix} - \hat{x}_{k|k-1})$;

d. Update error covariance, $P_k = (I - K_k)P_{k-1} + Q$;

e. Update P_k ensuring $P_k \geq P_{min}$ by $\max(P_k, P_{min})$;

f. Store state estimates, $reconstructed\_signal(k) = \hat{x}_k$;

end for

3: Return reconstructed signal $\hat{x}$.

Algorithm 1. Adaptive Kalman filter for respiratory and heartbeat signal reconstructionExperimentation and evaluation

Experimental parameters and settings

The experimental equipment used in this paper is the IWR1642BOOST radar and the DCA1000EVM data acquisition board for the acquisition of the human life signals and the synchronized heart rate monitoring using the HUAWEI WATCH GT2 as a reference ground truth. The IWR1843 is a single-chip millimeter-wave radar sensor that operates in the 76–81 GHz frequency band. The radar has three transmitter antennas and four receiving antennas. The experiment was conducted in an office scenario, as shown in Fig. 9a. This preliminary experiment used six subjects to conduct a comparative analysis of the methods in order to assess their accuracy. The basic information of the participants is shown in Table 4. All subjects were fully informed and consented to participate in this study.

During the experiment, the IWR1843BOOST millimeter-wave radar and the DCA1000EVM data acquisition board were placed directly in front of the target under test to acquire the raw ADC data and transmit the data to the computer via a USB data cable. When the computer receives the raw data, based on the hardware configuration of AMD Ryzen 7 5800H and 16G RAM, MATLAB is used to parse and process the raw data, and the radar setup parameters are shown in Table 5.

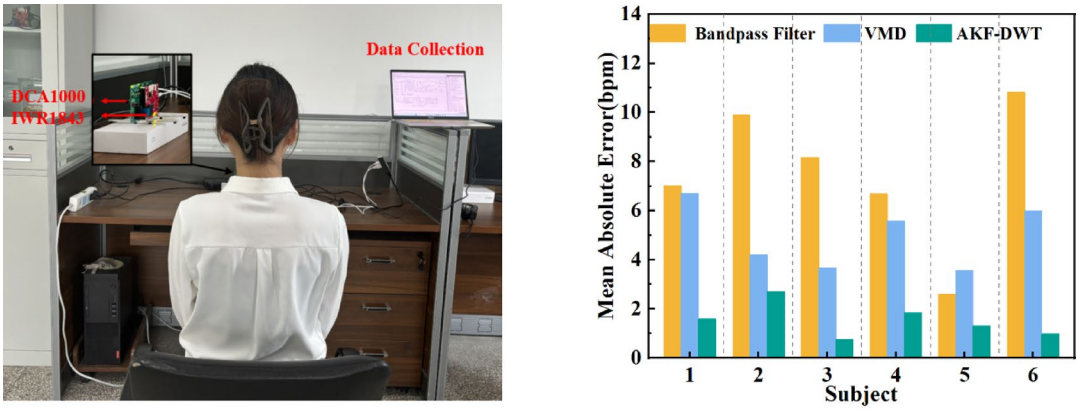

Fig. 9. (**a**) Experimental setup (**b**) Mean estimation errors for three methods for six subjects. (the·person·in·(**a**)·is author of this study).

Subject	Gender	Age	Height (cm)	Weight (kg)
1	Male	36	173	58
2	Female	26	158	44
3	Male	25	185	75
4	Male	24	180	85
5	Female	25	163	47
6	Female	23	160	50

Table 4. Basic information about the subjects.

Parameters	Value
Start frequency	77 GHZ
Bandwidth	4 GHZ
Number of transmitting antennas	1
Number of receiving antennas	4
Samples per-chirp	200
Chirp duration	50 μs
Frame duration	50 ms
Chirps per-frame	2

Table 5. Radar parameter setting.

This experiment was conducted after obtaining approval from the Ethics Committee of the Northwestern Normal University. The Ethics Review Committee of Northwest Normal University confirms that the project involving the use of millimeter wave radar technology for non-invasive monitoring of human respiration and heartbeat does not require further ethical review. All methods performed were in accordance with relevant guidelines and regulations, and informed consent was obtained from all subjects.

Mean absolute error (MAE) and mean absolute percentage error (MAPE) were used as metrics to evaluate the accuracy of heart rate estimation.

$$MAE = \frac{1}{N}\sum_{i=1}^{N}|H_r[i] - H_e[i]| \tag{13}$$

The MAPE is defined as:

$$MAPE = \frac{1}{N}\sum_{i=1}^{N}\frac{|H_r[i] - H_e[i]|}{H_r[i]} \times 100\% \tag{14}$$

where N is the total number of time windows, H_e is the estimated heart rate, and H_r is the heart rate reference value.

Overall performance

This section aims to evaluate the accuracy and reliability of the proposed method for heart rate estimation by comparing its performance with other commonly used techniques. Filtering, mode decomposition, and wavelet decomposition are the three most widely used methods for separating physiological signals. Therefore, we selected a band-pass filter and Variational Mode Decomposition (VMD) as representative methods for comparison with the proposed approach. First, the band-pass filter was configured with a frequency range of 0.8 Hz to 2 Hz to extract the heart rate signal. On the other hand, the VMD method decomposes the signal into multiple intrinsic mode functions (IMF), relying on frequency band separation to extract the primary heartbeat component. The specific parameters for VMD include setting the number of modes K to 4, the penalty factor ∂ to 2000, and the tolerance τ to $1e^6$.

By comparing the Mean Absolute Error (MAE) and Mean Absolute Percentage Error (MAPE) of the three methods, we can assess their performance. Figure 9b shows the absolute error in heart rate estimation for six subjects using the three methods, while the detailed MAPE and MAE results are listed in Table 6. The results indicate that the estimation error for the band-pass filter ranges from 2.67 to 16.6%, while VMD yields an error range of 4.27% to 10.48%. In contrast, the proposed method achieves a smaller error range of 1.85% to 4.78%. Furthermore, we conducted additional experiments under varying distances, angles, breathing methods, and postures to validate the proposed method's effectiveness further. These experimental results demonstrate that the proposed method exhibits high reliability and accuracy across multiple scenarios, highlighting its potential for practical applications.

Subject	Bandpass filter	VMD	AKF-DWT
1	6.72	8.52	2.94
2	9.09	4.69	3.14
3	8.57	4.27	1.85
4	4.82	10.48	2.08
5	2.67	5.48	4.78
6	16.6	7.05	2.80

Table 6. Three methods of MAPE.

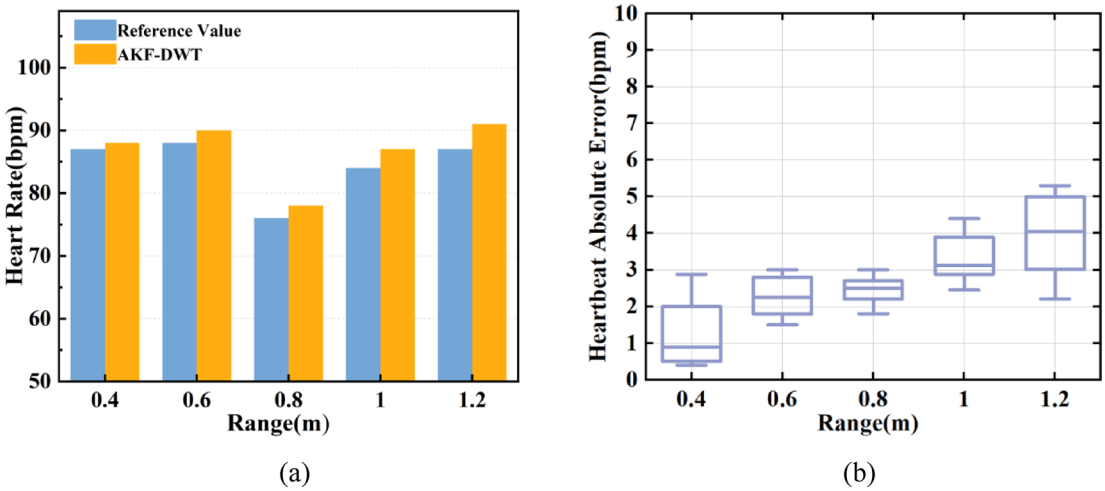

Fig. 10. Different distances (**a**) Reference and estimated values (**b**) Absolute error value of heart rate estimation.

Different impact factors

In order to verify the performance of the MRVS method in different settings, relevant experiments regarding distance, angle, and breathing methods are conducted in this section.

Different distances

This section of the experiment investigated the effect of the distance between the radar and the subject on heart rate estimation accuracy. With the radar's angle and height relative to the subject's chest kept constant, the distance between the subject and the radar was gradually increased from 0.4 to 1.2 m in 0.2 m increments, and heart rate estimation results were obtained at five different distances. Figure 10a presents the heart rate estimation results at these distances. The experimental results demonstrate that heart rate estimation error gradually increases as the distance grows, which is attributed to accelerated signal attenuation, leading to reduced estimation accuracy. However, despite the increased error at a distance of 1.2 m, the error remains within 5%. Figure 10b illustrates the recognition accuracy across different distances. As the distance increases, the absolute error in heart rate estimation consistently stays within 4 bpm, indicating that the proposed method offers strong stability in heart rate estimation over a broad range of distances.

Different angles

This section of the experiment was designed to investigate the effect of the incidence angle on heart rate monitoring accuracy. In the experiment, subjects were positioned at a fixed distance of 0.8 m from the radar device, while the incidence angle was gradually increased from 0° to 45° in 15° increments. Figure 11a illustrates the number of heart rate estimations at different angles, and Fig. 11b shows the absolute error of the heart rate at these angles. The experimental results indicate that heart rate estimation error increases significantly with larger incidence angles. The mean absolute percentage errors (MAPE) at the four angles were 1.65% at 0°, 3.95% at 15°, 5.84% at 30°, and 6.89% at 45°. As the incidence angle increases, the mean absolute error (MAE) also increases, corresponding to a gradual decline in monitoring accuracy. This is because the effective reflective area decreases with larger angles, reducing heart rate monitoring accuracy. Nevertheless, the MRE remained below 7% at an angle of up to 45°, indicating that the proposed method maintains relatively strong stability across a wide range of incidence angles.

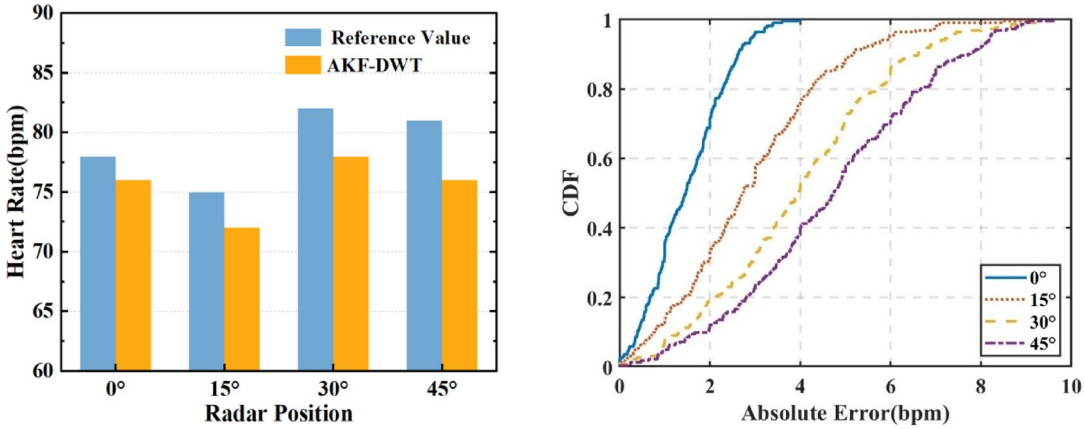

Fig. 11. Different angles (**a**) Reference and estimated values (**b**) CDF.

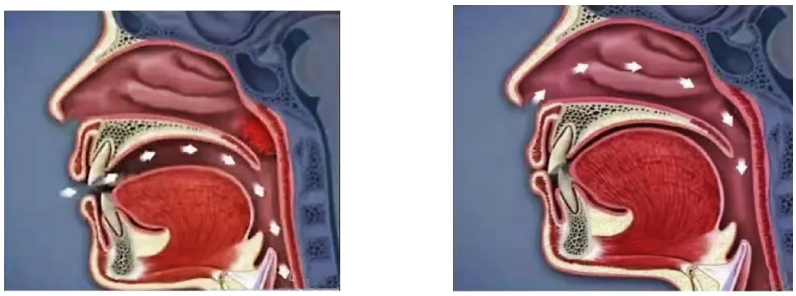

Fig. 12. Principles of breathing (**a**) oral breathing (**b**) nasal breathing.

Different respiratory patterns

This study aimed to investigate the physiological effects of oral versus nasal breathing on heart rate in greater depth. The experiment involved six healthy adult subjects, including two patients with chronic rhinitis who were more accustomed to mouth breathing. This was done to avoid abrupt changes in breathing patterns that could influence heart rate. Figure 12 illustrates the different breathing patterns used in the experiment. Throughout the study, the subjects maintained a distance of 0.8 m from the radar, which was positioned directly in front of their chests. The experiment required subjects to remain calm and relaxed, ensuring that the number of oral and nasal breaths taken during the session was equal for each participant.

Figure 13a shows the heart and respiratory rates under different breathing styles. The experiment showed that the subjects' heart rate when they adopted oral breathing was about six bpm higher than that of nasal breathing, consistent with the experiment's results in six subjects, including two chronic rhinitis patients. The reason for this may be that mouth breathing increases the activity of the sympathetic nervous system, which leads to an increase in heart rate, and that the air cannot be filtered when breathing through the mouth, so if mouth breathing is used for an extended period, it not only affects the appearance of the face but also may cause cardiopulmonary diseases[39, 40].

Figure 13b presents the mean estimation error for oral and nasal breathing across the six subjects. The estimation error for oral breathing is notably higher than that for nasal breathing. This discrepancy may be due to the smoother and larger thoracic vibrations produced during nasal breathing, which are easier to detect. In contrast, oral breathing may introduce random body movements, leading to reduced estimation accuracy.

Different postures

This section of the experiment was designed to systematically assess the effect of heart rate estimation in subjects in the seated, standing, and back-to-standing states. To further evaluate the robustness of the proposed method across varying scenarios, an additional six healthy subjects between the ages of 25 and 35 were recruited, and a heart rate monitoring device was used to record heart rate data in the three states. Based on the experiment results in 4.3.1 and the customary distance of people sitting and standing daily, 0.8 m was chosen as the experimental distance for this part.

During the experiment, each subject was monitored for 1 min in the state of sitting upright, standing upright, and back-to-standing. We decomposed the heart rate in different states by the proposed method and analyzed

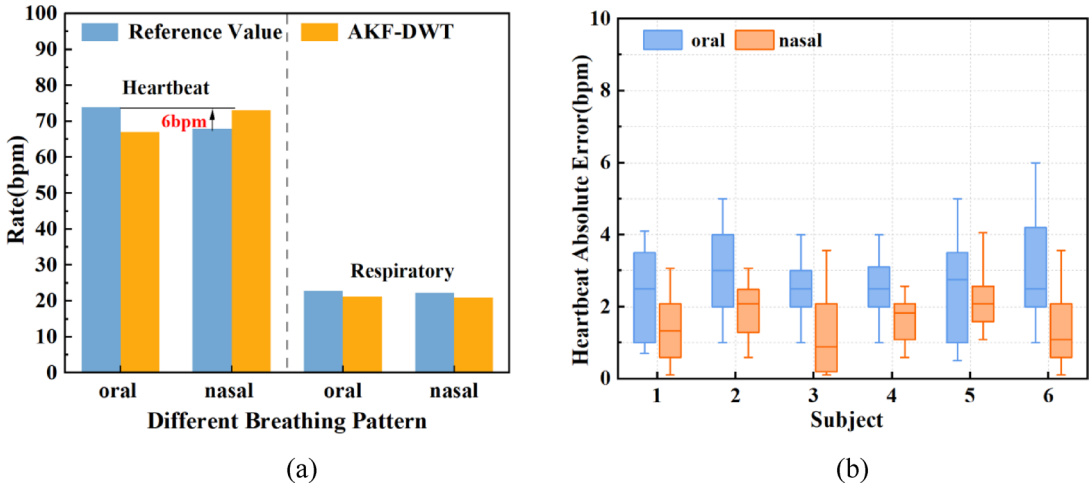

Fig. 13. Different respiratory patterns (**a**) Reference and estimated values (**b**) MAE of heart rate for six subjects.

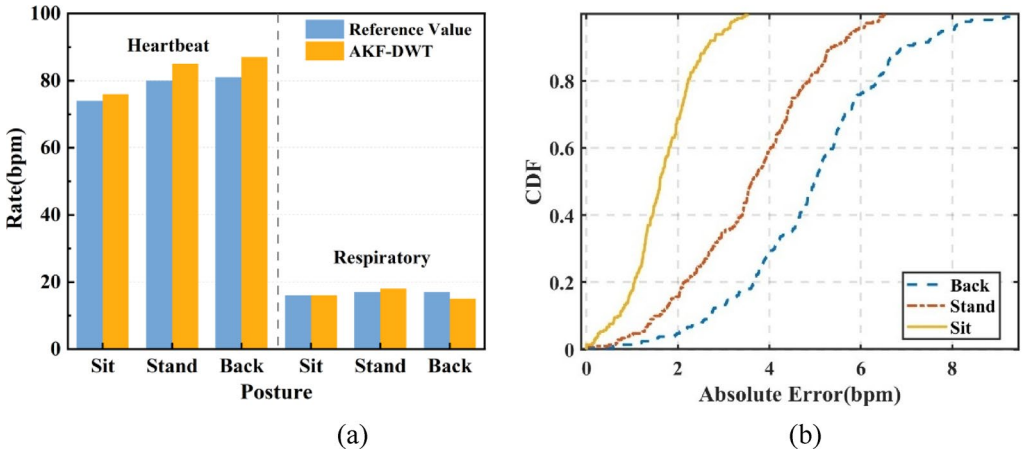

Fig. 14. (**a**) Heart rate and respiratory reference values and estimates (**b**) CDF.

the estimation results such as Fig. 14a demonstrates the respiration and heart rate estimation values versus the reference values, and Fig. 14b shows the cumulative distribution function of the absolute error of heart rate estimation in three different postures, with the highest error value of 4 bpm for the sitting-standing state, 7 bpm for the standing, and 9 bpm for the back-to-standing. Considering the MAPE results, it can be observed that the heart rate is lower in the seated position compared to the standing position. Additionally, the error rate for heart rate estimation in the standing position is 5.13%, which is 2.19% higher than that in the seated position. The reason for this is that the body will produce random movements when standing, which leads to poor estimation; in addition, the estimation error rate in the back-to-back standing state is 6.17%, which is slightly lower than that in the front-to-front standing state, which is because the amplitude of the chest caused by respiration and heartbeat is much larger than that of the back. The muscular structure of the back may make the signals more dispersed, which increases the difficulty of extracting the heart rate. However, more samples and in-depth analyses are needed to ensure substantial differences.

Comparison with recent research work

We compared the method proposed in this study with similar work, and the results are shown in Table 7. The results show that the method shows a lower Maximum Absolute Error Percentage (MAPE) at all testing distances, which is significantly better than the compared methods. Specifically, the method used in[28] showed an MAPE of 5.56% at a testing distance of 0.8 m, whereas in this study, the MAPE decreased to 4.59% at a testing distance of 1.2 m. In addition, although Wang et al.[41] achieved an MAPE of 2.57% at a monitoring distance of 0.6 m, the present study's method maintained high accuracy over a wider range of distances. Compared with the method using Composite Empirical Modal Decomposition (CEEMDAN)[42], the MAPE of this study's method was reduced to 3.57% at the same testing distance of 1 m. Although Liu et al.[37] also achieved a more accurate

Ref	Radar	Method	Distance (m)	MAPE (%)
[28]	AWR1642	SG Filter, FFT	0.8	5.56
[40]		VISION	0.6	2.57
[41]		CEEMDAN	1	4.38
[37]	IWR1642	WPD、WAAC	0.5–2.5 m	1.83–5.01
This Work	IWR1843	AKF-DWT	0.4–1.2	1.85–4.59

Table 7. Comparison with recent research work.

estimation over a wider range of distances, this study utilized the Discrete Wavelet Transform (DWT) with downsampling, effectively reducing the computational cost.

In summary, by combining Adaptive Kalman Filtering (AKF) and Discrete Wavelet Transform (DWT), the method in this study shows higher efficiency and accuracy in dealing with motion disturbances and signal decomposition. It can maintain high accuracy, especially when performing heart rate monitoring in complex environments.

Conclusion

This paper presents an innovative millimeter-wave radar-based vital signs monitoring method, MRVS. The processing flow includes three parts: signal enhancement, signal decomposition, and reconstruction, which realize the non-contact monitoring of respiratory and heartbeat signals. A signal enhancement technique combining signal superposition and first-order time differencing is proposed to highlight the chest displacement signal caused by heartbeat motion effectively. Meanwhile, the signal decomposition and reconstruction using Discrete Wavelet Transform (DWT) and Adaptive Kalman Filter (AKF) effectively suppress the clutter and noise and improve heart rate estimation accuracy. The experimental results show that the MRVS method performs well in estimating heart rate at different distances, angles, breathing modes, and postures, with an error rate of less than 7%. Accurately acquiring respiration and heart rate signals provides strong support for applications in fields such as non-contact medicine and smart homes but also uses the uniqueness of respiration and heart rate to achieve identification and personalized health monitoring, which can be the goal of our next research.

Data availability

The datasets generated during and/or analyzed during the current study are not publicly available due to [Data and processing information related to product development] but are available from the corresponding author on reasonable request.

Received: 23 July 2024; Accepted: 25 June 2025
Published online: 01 August 2025

References

1. Zhao, H. et al. Noncontact physiological dynamics detection using low-power digital-IF Doppler radar. *IEEE Trans. Instrum. Meas.* **66**(7), 1780–1788 (2017).
2. Piuzzi, E., Pisa, S., Pittella, E., Podestà, L. & Sangiovanni, S. Wearable belt with built-in textile electrodes for cardio—Respiratory monitoring. *Sensors* **20**(16), 4500 (2020).
3. Attia, Z. I. et al. An artificial intelligence-enabled ECG algorithm for the identification of patients with atrial fibrillation during sinus rhythm: A retrospective analysis of outcome prediction. *Lancet* **394**(10201), 861–867 (2019).
4. Lázaro, J. et al. Electrocardiogram derived respiratory rate using a wearable armband. *IEEE Trans. Biomed. Eng.* **68**(3), 1056–1065 (2020).
5. Guo, X., Guo, S., Zhao, Y. & Shi, J. Research on the key technology of non-contact vital signs monitoring. In *2023 6th International Conference on Computer Network, Electronic and Automation (ICCNEA)* 249–253. (IEEE, 2023).
6. Mignanelli, L., & Rembe, C. Non-contact health monitoring with LDV. In *Laser Doppler Vibrometry for Non-Contact Diagnostics* 1–8 (2020).
7. Nikitchuk, T. M. et al. Non-contact photoplethysmographic sensors for monitoring students' cardiovascular system functional state in an IoT system. *J. Edge Comput.* **1**(1), 17–28 (2022).
8. Eder, Y. & Eldar, Y. C. Sparsity-based multi-person non-contact vital signs monitoring via FMCW radar. *IEEE J. Biomed. Health Inform.* **27**(6), 2806–2817 (2023).
9. Han, Y., Lauteslager, T., Lande, T. S. & Constandinou, T. G. UWB radar for non-contact heart rate variability monitoring and mental state classification. In *2019 41st Annual International Conference of the IEEE Engineering in Medicine and Biology Society (EMBC)* 6578–6582. (IEEE, 2019).
10. Zhang, J., Xiao, W. & Li, Y. Data and knowledge twin driven integration for large-scale device-free localization. *IEEE Internet Things J.* **8**(1), 320–331 (2020).
11. Liu, X., Cao, J., Tang, S., Wen, J. & Guo, P. Contactless respiration monitoring via off-the-shelf WiFi devices. *IEEE Trans. Mob. Comput.* **15**(10), 2466–2479 (2015).
12. Zeng, Y. et al. MultiSense: Enabling multi-person respiration sensing with commodity wifi. *Proc. ACM Interact. Mob. Wear. Ubiquitous Technol.* **4**(3), 1–29 (2020).
13. Li, C., Lin, J. & Xiao, Y. Robust overnight monitoring of human vital signs by a non-contact respiration and heartbeat detector. In *2006 International Conference of the IEEE Engineering in Medicine and Biology Society* 2235–2238. (IEEE, 2006).
14. Dong, S. et al. Doppler cardiogram: A remote detection of human heart activities. *IEEE Trans. Microw. Theory Tech.* **68**(3), 1132–1141 (2019).
15. Hosseini, S. A. T., & Amindavar, H. UWB radar signal processing in measurement of heartbeat features. In *2017 IEEE International Conference on Acoustics, Speech and Signal Processing (ICASSP)* 1004–1007. (IEEE, 2017).

16. Muñoz-Ferreras, J. M., Wang, J., Peng, Z., Gómez-García, R. & Li, C. From Doppler to FMCW radars for non-contact vital-sign monitoring. In *2018 2nd URSI Atlantic Radio Science Meeting (AT-RASC)* 1–4. (IEEE, 2018).
17. Gu, C., Wang, G., Inoue, T. & Li, C. Doppler radar vital sign detection with random body movement cancellation based on adaptive phase compensation. In *2013 IEEE MTT-S International Microwave Symposium Digest (MTT)* 1–3. (IEEE, 2013).
18. Lee, H., Kim, B. H., Park, J. K. & Yook, J. G. A novel vital-sign sensing algorithm for multiple subjects based on 24-GHz FMCW Doppler radar. *Remote Sens.* **11**(10), 1237 (2019).
19. Alizadeh, M., Shaker, G., De Almeida, J. C. M., Morita, P. P. & Safavi-Naeini, S. Remote monitoring of human vital signs using mm-wave FMCW radar. *IEEE Access* **7**, 54958–54968 (2019).
20. Alafeef, M. & Fraiwan, M. Smartphone-based respiratory rate estimation using photoplethysmographic imaging and discrete wavelet transform. *J. Amb. Intell. Human. Comput.* **11**, 693–703 (2020).
21. Koyanaka, R., Sato, S., Hu, Y. & Toda, T. A study on pre-filter design for improving accuracy in heart rate estimation from backside using discrete wavelet transform with mm-wave radar. *IEICE Commun. Express* **10**(12), 1009–1014 (2021).
22. Ding, Y. et al. A novel real-time human heart rate estimation method for noncontact vital sign radar detection. *IEEE Access* **8**, 88689–88699 (2020).
23. Ji, S., Wen, H., Wu, J., Zhang, Z. & Zhao, K. Systematic heartbeat monitoring using a fmcw mm-wave radar. In *2021 IEEE International Conference on Consumer Electronics and Computer Engineering (ICCECE)* 714–718. (IEEE, 2021).
24. Islam, S. M., Motoyama, N., Pacheco, S. & Lubecke, V. M. Non-contact vital signs monitoring for multiple subjects using a millimeter wave FMCW automotive radar. In *2020 IEEE/MTT-S International Microwave Symposium (IMS)* 783–786. (IEEE, 2020).
25. Kim, H. J., Kim, K. H., Hong, Y. S. & Choi, J. J. Measurement of human heartbeat and respiration signals using phase detection radar. *Rev. Sci. Instrum.* **78**(10), 64 (2007).
26. Van Loon, K. et al. Wireless non-invasive continuous respiratory monitoring with FMCW radar: A clinical validation study. *J. Clin. Monit. Comput.* **30**, 797–805 (2016).
27. Anitori, L., de Jong, A. & Nennie, F. FMCW radar for life-sign detection. In *2009 IEEE Radar Conference* 1–6. (IEEE, 2009).
28. Riahi, T. A. R. I. Q. Contactless Heartbeat Estimation with FMCW Radar (Bachelor's thesis, University of Twente) (2024).
29. Huang, N. E. et al. The empirical mode decomposition and the Hilbert spectrum for nonlinear and non-stationary time series analysis. *Proc. Roy. Soc. Lond. Ser. Math. Phys. Eng. Sci.* **454**(1971), 903–995 (1998).
30. Djelaila, S., Berrached, N. E., Chalabi, Z. & Taleb-Ahmed, A. The diagnosis of cardie arrhythmias using heart rate variability analysis by the EMD. In *2016 8th International Conference on Modelling, Identification and Control (ICMIC)* 822–825. (IEEE, 2016).
31. Dragomiretskiy, K. & Zosso, D. Variational mode decomposition. *IEEE Trans. Signal Process.* **62**(3), 531–544 (2013).
32. Yang, D., Zhu, Z. & Liang, B. Vital sign signal extraction method based on permutation entropy and EEMD algorithm for ultra-wideband radar. *IEEE Access* **7**, 178879–178890 (2019).
33. Shen, H. et al. Respiration and heartbeat rates measurement based on autocorrelation using IR-UWB radar. *IEEE Trans. Circuits Syst. Express Briefs* **65**(10), 1470–1474 (2018).
34. Xu, X., Yu, J., Ma, C., Ren, Y., Liu, H., Zhu, Y. & Tang, F. mmECG: Monitoring human cardiac cycle in driving environments leveraging millimeter wave. In *IEEE INFOCOM 2022-IEEE Conference on Computer Communications* 90–99. (IEEE, 2022).
35. He, M., Nian, Y. & Liu, B. Noncontact heart beat signal extraction based on wavelet transform. In *2015 8th International Conference on Biomedical Engineering and Informatics (BMEI)* 209–213. (IEEE, 2015).
36. Wang, Y., Wang, W., Zhou, M., Ren, A. & Tian, Z. Remote monitoring of human vital signs based on 77-GHz mm-wave FMCW radar. *Sensors* **20**(10), 2999 (2020).
37. Liu, L., Zhang, S. & Xiao, W. Noncontact vital signs detection using joint wavelet analysis and autocorrelation computation. *Chin. J. Eng.* **43**(9), 1206–1214 (2021).
38. Xu, Y. Research on non-contact health monitoring system based on millimeter-wave radar. Doctoral dissertation, University of Electronic Science and Technology of China (2022).
39. Krasowski, J. A. *Breath, The New Science of a Lost Art: by James Nestor* 304 (Riverhead Books, 2020).
40. Zhao, Z. et al. Effects of mouth breathing on facial skeletal development in children: A systematic review and meta-analysis. *BMC Oral Health* **21**, 1–14 (2021).
41. Wang, Y. et al. A novel non-contact respiration and heartbeat detection method using frequency-modulated continuous wave radar. *IEEE Sens. J.* **24**, 10434–10446 (2024).
42. Lv, W. et al. Remote measurement of short-term heart rate with narrow beam millimeter wave radar. *IEEE Access* **9**, 165049–165058 (2021).

Author contributions

Conceptualization, Z.H. and Y.W.; methodology, Y.W.; software, Y.W.; validation, G.D., K.F. and Y.G.; formal analysis, Y.W.; investigation, Z.H.; data curation, Y.W.; writing—original draft prepa-ration, Y.W.; writing—review and editing, Z.H. and F.L.; supervision, Z.H.; project administration, Z.H.; funding acquisition, Z.H. All authors have read and agreed to the published version of the man.

Funding

This work was supported by the National Natural Science Foundation of China (Grant 62262061, Grant 62162056, Grant 62261050), Major Science and Technology Projects of Gansu (23ZDGA009), Science and Technology Commissioner Special Project of Gansu (23CXGA0086), Lanzhou City Talent Innovation and Entrepreneurship Project (2020-RC-116, 2021-RC-81), and Gansu Provincial Department of Education: Industry Support Program Project (2022CYZC-12), Northwest Normal University Young Teachers Research Ability Enhancement Program Project (NWNU-LKQN2019-28).

Declarations

Competing interests

The authors declare no competing interests.

Ethics approval and consent to participate

The Ethics Review Committee of Northwest Normal University confirms that the project involving the use of millimeter wave radar technology for non-invasive monitoring of human respiration and heartbeat does not require further ethical review. This project does not involve invasive procedures on participants, nor does it involve the collection or processing of sensitive data. Therefore, in accordance with the Declaration of

Helsinki and other applicable ethical guidelines, the design of this research project meets ethical standards. All participants have provided informed consent, and measures are in place to ensure data anonymization and privacy protection. The committee has determined that this project does not present ethical risks.

Additional information

Correspondence and requests for materials should be addressed to Z.H.

Reprints and permissions information is available at www.nature.com/reprints.

Publisher's note Springer Nature remains neutral with regard to jurisdictional claims in published maps and institutional affiliations.